Chemical Physics 373 (2010) 90-97

http://dx.doi.org/10.1016/j.chemphys.2010.02.006

β-carotene to bacteriochlorophyll *c* energy transfer in self-assembled aggregates mimicking chlorosomes

J. Alster[a], T. Polívka[b,c], J. B. Arellano[d], P. Chábera[b], F. Vácha[b,c], J. Pšenčík[a,b,*]

[a]Faculty of Mathematics and Physics, Charles University, Ke Karlovu 3, 121 16 Praha, Czech Republic

[b]Institute of Physical Biology, University of South Bohemia, Zámek 136, 373 33 Nové Hrady, Czech Republic

[c]Biology Centre, Academy of Sciences of the Czech Republic, Branišovská 31, 370 05 České Budějovice, Czech Republic

[d]Instituto de Recursos Naturales y Agrobiología de Salamanca (IRNASA-CSIC), Apdo. 257, 37071 Salamanca, Spain

[*]corresponding author; e-mail: psencik@karlov.mff.cuni.cz, tel.: (+420) 221 911 248, fax: (+420) 221 911 249

Keywords: chlorosomes; bacteriochlorophyll aggregates; β-carotene; excitation energy transfer; femtosecond spectroscopy

Abstract

Carotenoids are together with bacteriochlorophylls important constituents of chlorosomes, the light-harvesting antennae of green photosynthetic bacteria. Majority of bacteriochlorophyll molecules form self-assembling aggregates inside the chlorosomes. Aggregates of bacteriochlorophylls with optical properties similar to those of chlorosomes can also be prepared in non-polar organic solvents or in aqueous environments when a suitable non-polar molecule is added. In this work, the ability of β-carotene to induce aggregation of bacteriochlorophyll *c* in aqueous buffer was studied. Excitation relaxation and energy transfer in the carotenoid-bacteriochlorophyll assemblies were measured using femtosecond and nanosecond transient absorption spectroscopy. A fast, ~100-fs energy transfer from the S_2 state of β-carotene to bacteriochlorophyll *c* was revealed, while no evidence for significant energy transfer from the S_1 state was found. Picosecond formation of the carotenoid triplet state (T_1) was observed, which was likely generated by singlet homo-fission from the S_1 state of β-carotene.

Introduction

Chlorosomes of green photosynthetic bacteria are the most efficient light-harvesting complexes in Nature [1]. In addition, chlorosomes differ from other photosynthetic complexes in that they lack a protein scaffold housing pigments. Instead, bacteriochlorophyll (BChl) *c*, *d* or *e* molecules found in the interior of the chlorosome are present in the form of self-organized aggregates [2,3]. Proteins are located only in the chlorosome baseplate and envelope [4,5]. Other constituents of chlorosomes are lipids, quinones, and carotenoids [2,3]. Lipids are probably part of the chlorosome envelope, together with proteins [6,7]. Quinones are involved in a protective redox-dependent excitation energy quenching mechanism [8], while carotenoids have both light harvesting and photoprotective functions [9-15]. Singlet excitation energy transfer from carotenoid to aggregated BChls with efficiency between 50 and 80% has been determined in chlorosomes [9,12,14]. The dominant energy transfer pathway proceeds via the carotenoid S_2 state with a fast rate constant of ~$(100\ fs)^{-1}$ [14]. In addition, it was suggested that carotenoids are important for the biogenesis of the chlorosome baseplate and its attachment to the cytoplasmic membrane [16,17].

BChl aggregates are organized in curved lamellar structures in chlorosomes [18-21]. Relatively polar chlorin rings of BChls assemble into lamellar layers via several specific interactions; however, the actual molecular arrangement is still a matter of debate [21-23]. The lamellar layers held together by hydrophobic interactions between interdigitated esterifying alcohols of BChls [18,24]. The hydrophobic space between the chlorin layers is occupied by carotenoids and quinones, together with esterifying alcohols [19].

Self-organized aggregates of chlorosomal BChls with spectral properties similar to those of chlorosomes can be prepared also in-vitro (for review, see [25,26]). This can be achieved either in a non-polar environment, where the aggregation is driven by hydrophilic interactions between polar heads of BChls, or in a polar environment (e.g. aqueous buffer), where the aggregation is driven by hydrophobic interactions between esterifying alcohol tails of BChls [27,28]. Addition of suitable non-polar molecules is necessary to induce aggregation in aqueous solutions, most likely because hydrophobic interactions between farnesyl tails of BChl *c* molecules alone are not sufficiently strong to drive it [24]. Lipids [29,30], quinones with a hydrophobic side chain [31], and chlorosomal carotenoid chlorobactene [24] were shown to have such an inducing effect on BChl *c* aggregation. In addition, synthetic surfactants [32,33] and hydrophobic mixture of silanes [34] induced aggregation of synthetic zinc chlorins. It is interesting to note that the main constituents of chlorosomes of green sulfur bacteria are in the above list. The selected aggregation-inducing molecules affect properties of

the resulting aggregates. For example, aggregates of BChl *c* and quinones exhibit redox-dependent quenching of the excitation energy [31]. Light-harvesting efficiency, self-assembly, and stability make aggregates of chlorosomal BChls and their synthetic analogs promising materials for artificial photosynthesis [35-38].

Chlorosomes of green sulfur bacteria contain mainly aryl carotenoids with a ϕ-end-group (chlorobactene, isoerenieratene, Figure 1) [3]. Chlorobactene was shown to induce aggregation of BChl *c* in aqueous solutions [24], however, it remains unclear whether this ability is a general property of all non-polar carotenoids, or it is affected by their end groups. For example, chlorosomes of green filamentous bacterium *Chloroflexus aurantiacus* contain three main carotenoids without a ϕ-end-group: β-carotene, γ-carotene, and OH-γ-carotene glucoside [39]. In this work we studied whether β-carotene (Figure 1) is able to induce aggregation. In addition, energy transfer dynamics of the final assemblies was investigated by means of transient absorption spectroscopy and compared with data available for chlorosomes.

2. Materials and methods

2.1. Self-assembly experiments

BChl *c* was isolated from green sulfur bacterium *Chlorobaculum tepidum* (formerly known as *Chlorobium tepidum*) as described previously [24]. All four main homologs of BChl *c* were pooled together, in the same ratio as they were isolated from chlorosomes. β-carotene was purchased from Fluka. Aggregates of BChl *c* and β-carotene were prepared as follows: BChl *c* was dissolved in methanol, and β-carotene in acetone or tetrahydrofuran (THF). THF was used in experiments that required high concentrations of β-carotene in the sample. The solvents containing β-carotene and BChl *c* were mixed in various ratios to get a final molar ratio of β-carotene to BChl *c* within 0.1-1.4:1 range. This mixture was then injected into stirred 50 mM Tris-HCl pH 8.0 buffer. The final concentration of organic solvent did not exceed 2%. The final concentration of BChl *c* in the buffer was approximately 20 μM for self-assembly experiments and ~200 μM for transient absorption spectroscopy. Sample concentrations were determined from absorption spectra, using the extinction coefficients of 70 $mM^{-1}cm^{-1}$ for BChl *c* in methanol at the Q_y maximum [40] and 139 $mM^{-1}cm^{-1}$ for β-carotene in both acetone and THF at the absorption maximum [41,42]. It should be noted that the reported molar ratios were determined for initial mixtures. It is possible that a small fraction of the β-carotene molecules was not incorporated into the BChl *c* aggregates and precipitated in the buffer. Samples were left overnight in dark at room temperature to reach

stable steady-state absorption spectra. Steady-state absorption spectra were measured using Specord 250 spectrometer (Analytic Jena).

2.2. Time-resolved spectroscopy

Femtosecond pulses used for the transient absorption measurement in fs-ps time range were provided by an amplified laser system Integra-i (Quantronix), consisting of Er-fiber oscillator and Ti:Sapphire amplifier, which produces ~130 fs pulses centered at 795 nm at a repetition rate of 1 kHz. The amplified pulses were divided into two paths serving as excitation and probe beams. Excitation pulses were obtained by directing a part of the amplifier output to the optical parametric amplifier (TOPAS, Light Conversion). The broadband white-light probe pulses were produced by focusing a fraction of the 795 nm beam to a 3 mm sapphire plate. The white-light pulses were further divided into the probe beam that overlapped with the excitation beam at the sample, and a reference beam. Both probe and reference beams were dispersed in a spectrograph onto a double photodiode array with 1024 elements allowing measurements of transient spectra in a spectral window of ~240 nm. In all measurements the mutual polarization of pump and probe beams was set to the magic angle (54.7˚) by placing a polarization rotator in the pump beam. All measurements were carried out in a rotating cuvette consisting of two 1 mm quartz windows separated by a 1 mm Teflon spacer to prevent sample degradation during the measurements. Excitation intensities of $\sim 5 \times 10^{14}$ photons $pulse^{-1}$ cm^{-2} (720 nm) and $\sim 10^{15}$ photons $pulse^{-1}$ cm^{-1} (490-520 nm) were used, except the experiments where intensity dependence of the kinetics was studied. Steady-state absorption spectra were measured before and after the experiments to ensure that no degradation occurred during the data acquisition.

For transient absorption spectroscopy in ns-μs timescale, samples were excited at 535 nm with ~5 ns pulses (energy ~5 mJ) from an optical parametric oscillator (PG122, EKSPLA) pumped by a Q-switched Nd:YAG laser (NL303G/TH, EKSPLA). Xenon flash lamp (XE 2000, Avantes) was used as the source for the probe and reference pulses. Signal was detected by an intensified CCD camera (PI-MAX 512RB, Roper Scientific), with a 5 ns gate-width, coupled to an imaging spectrometer (Triax 320, Horiba Jobin Yvon). Transient absorption spectra were measured with right angle geometry in fluorescence glass cuvettes with 1 cm path length and averaged from 1000 flashes. Both femtosecond and nanosecond experiments were performed at aerobic conditions.

Transient absorption was analyzed by both single-kinetic and global fitting [43]. The data were fitted to a sum of exponentials. Results of global analysis are shown as decay

associated spectra (DAS), which represent spectral profiles of the pre-exponential factors of the lifetime components. Characteristic lifetimes are reported with an error not exceeding 20%.

3. Results

3.1. Aggregate formation

Figure 2a shows steady-state absorption spectra of BChl *c* and β-carotene aggregates with several molar ratios between BChl *c* and β-carotene. Pure BChl *c* is partially soluble in aqueous buffer, where it forms dimers with the Q_y band peaking at 710 nm [24,44]. Upon the injection of the BChl *c* and β-carotene mixture into buffer, a spectral red shift of the BChl *c* Q_y band is observed, which increases with increasing β-carotene to BChl *c* molar ratio. The ratio of approximately 0.3:1 leads to a shift of the Q_y band of BChl *c* beyond 715 nm, and the highest molar ratio used in this study, 1.4:1, induces a shift to 729 nm. Since the red shift is an indication of the formation of BChl *c* aggregates [3], the results clearly show that β-carotene induces aggregation of BChl *c* in aqueous buffer. Moreover, the data shown in Figure 2c provide evidence that β-carotene molecules are inside the BChl *c* aggregates. When pure β-carotene is injected into the buffer, a blue shift of the absorption spectrum is observed in respect of that in THF. In contrast, a red-shift of the carotenoid absorption peak is observed upon injection of a mixture of β-carotene and BChl *c* (Figure 2b,c). In addition, β-carotene in aqueous buffer precipitates, whereas it remains stable in aggregates with BChl *c*.

3.2. Transient absorption

To study relaxation and energy transfer processes in the carotenoid-BChl assemblies, femtosecond transient absorption was measured. Time-resolved measurements were carried out with samples having an intermediate β-carotene to BChl *c* molar ratio of 0.3:1. Samples with higher β-carotene to BChl *c* molar ratio exhibited similar lifetimes and DAS; the only prominent difference was a red shift of the amplitudes associated with the relaxation of the Q_y band of BChl *c* (data not shown), reflecting the red shift of the Q_y band in the steady-state absorption spectra.

Three different excitation wavelengths were used, 490, 520 and 720 nm. Excitation at 720 nm was used to explore exciton interaction between β-carotene and BChl *c*. At this excitation wavelength only BChl *c* can be excited, but not β-carotene. If exciton coupling between carotenoid and BChl were present, a ground state bleaching of β-carotene would be observed after BChl excitation. However, the absence of a carotenoid bleaching around 550 nm (Figure

3) makes significant exciton interaction between β-carotene and BChl *c* unlikely, since a clear bleaching band is observed in this spectral region after carotenoid excitation (see below).

In order to monitor energy transfer and relaxation processes occurring after excitation of β-carotene (Figure 4a), we have recorded transient absorption data after excitation at 490 and 520 nm. The probability to excite β-carotene is maximal in this spectral region (Figure 2). By comparing absorption spectra of BChl *c* aggregates with and without β-carotene (Figure 2a) it can be estimated that at least 1-1.5 molecules of β-carotene were excited for every molecule of BChl *c*. This estimate does not account for scattering and possible spectral shift of the BChl *c* Soret band upon aggregation (see the Discussion).

Transient absorption spectra recorded at a few characteristic time delays after excitation at 520 nm are shown in Figure 4a. The data obtained after excitation at 490 nm were similar. The two dominating features, positive excited-state absorption band peaking at 580 nm and strong negative band centered around 740 nm, correspond to the S_1-S_n transition of β-carotene and bleaching of the BChl Q_y band, respectively. Both bands are fully developed within the first 500 fs, indicating that ultrafast energy transfer channel from the S_2 state of β-carotene is active in these aggregates. The transient signals in the whole spectral region decay on a timescale of a few picoseconds, but it is obvious that the decay of the S_1-S_n signal does not match that of the Q_y bleaching, suggesting a separate dynamics of β-carotene and BChl *c* relaxation.

Further insight into excited-state processes in aggregates was obtained by application of global fitting analysis. At least five time components were required to obtain a satisfactory fit. Figure 4b shows DAS obtained from fitting the data recorded after excitation at 520 nm. The fastest component has a ~100-fs lifetime and its DAS shows that it is connected with a decay of photobleaching-stimulated emission (PB/SE) signal of the S_2 state of β-carotene, that is accompanied by a concomitant rise of the signal in the spectral region of the Q_y band of BChl *c* aggregates. Therefore, this component clearly corresponds to the depopulation of the S_2 state of β-carotene via energy transfer to BChl *c*.

The next process occurring after the ultrafast energy transfer from β-carotene to BChl *c* is characterized by a lifetime of ~350 fs. The DAS of this component exhibits a negative amplitude in the blue part of the Q_y band of BChl *c* and a positive amplitude in its red part, indicating energy redistribution within the Q_y band of the aggregated BChl *c* (most likely exciton relaxation). In the carotenoid region, similar features, but with opposite wavy character, indicates vibrational cooling within the S_1 state of β-carotene [45].

The next two components are difficult to extract without adding constraints to the fitting

parameters, because the decay of the relaxed S_1 state of β-carotene and annihilation processes, which most likely occur within the aggregates [46], take place on similar timescales. Therefore, in order to obtain information about these processes separately, we have measured kinetics at maxima of the S_1-S_n and Q_y bands with excitation intensities varying between 3.2×10^{14} to 2×10^{15} photons pulse^{-1} cm^{-2}. The results depicted in Figure 5 clearly show that while no intensity dependence has been detected in the carotenoid region, changes characteristic of annihilation indeed occur in the BChl bleaching decays. Therefore caution is needed when fitting and interpreting kinetics in the BChl *c* spectral region. Single-wavelength fitting of the S_1-S_n decays yields the identical time component of 6 ps regardless the excitation intensity, clearly identifying this component as the lifetime of β-carotene.

Consequently, having established that the S_1 lifetime of β-carotene in aggregates is 6 ps, we have fixed this time component in the global fitting. Applying this constraint, the third component has a lifetime of ~3 ps and is most pronounced in the Q_y region of aggregated BChl *c*, where it is manifested as a decay of both excited state absorption (ESA) around 690 nm and PB/SE around 740 nm. This relaxation is ascribed to both singlet-singlet annihilation and energy transfer within BChl aggregates. The fourth component with a fixed 6 ps lifetime has dominating amplitude in the spectral region of the S_1-S_n transition of β-carotene, confirming the assignment obtained from the fitting of the single kinetics. Yet, this component also has an amplitude at the most red part of the BChl bleaching band, where it most likely also corresponds to annihilation that, as evidenced in Figure 5, takes place on a timescale comparable to the S_1-S_n decay. It must be noted, however, that when the constraint of fixing the 6 ps component is released, the global analysis yields ~3 ps and ~8 ps components, both of which exhibit spectra with a mixture of features of BChl and S_1 state of β-carotene (not shown). However, since the single kinetic fitting did not reveal any 8 ps lifetime, this component is likely the result of a mixture of excited state species and does not correspond to a true lifetime. To further support this conclusion, we have applied global analysis separately to the spectral regions of BChl (640-770nm) and carotenoid S_1-S_n band (540-640 nm). Such analysis yields components with ~3 ps and ~6.5 ps lifetimes in the BChl region, but reveals only a component with a ~5.5 ps lifetime in the carotenoid region (data not shown). These lifetimes agree well with the single-kinetic fits in the respective spectral regions. Indeed, fixing one of the lifetimes in the global analysis to 5.5-6.5 ps only leads to negligible changes in residuals, but untangles the decay associated spectra. Although the 3 ps and 6 ps lifetimes are very similar, both components have clearly different spectra (Figure 4b). Other components of the global analysis are not affected by fixing the 6 ps lifetime. Thus,

we conclude that the 6 ps component is the S_1 lifetime of β-carotene in aggregates, suggesting that it is slightly shortened in comparison with the S_1 lifetime of 9-11 ps obtained for β-carotene in organic solvents [47].

The last resolved component describes all relaxation processes with lifetimes beyond the measuring time window (45 ps). Part of its amplitude is due to relaxation of BChl *c* aggregates to the ultimate acceptor state of the assembly. However, this component is also associated with an ESA signal around 550 nm. To identify the origin of this long-lived component, we have measured transient absorption spectra at the ns-μs timescale. The data measured for the sample having a β-carotene to BChl ratio of 0.3:1 after excitation at 535 nm were fitted globally and DAS of the only component characterized by a 2.3 μs lifetime is shown in Figure 6. The spectral profile and lifetime of this component are characteristic of the β-carotene triplet state, e.g. in chlorosomes of *Chloroflexus aurantiacus* [12]. This indicates that, contrary to carotenoids in organic solvents whose yield of triplet formation is negligible, β-carotene in aggregates with BChl can produce triplets with significantly higher yield. Since the maximum of the T_1-T_n band shown in Figure 6 matches well the maximum of the long-lived component obtained from the global fitting of transient absorption data measured after femtosecond excitation (Figure 4), we assign the residual signal at 550 nm in Figure 4 to the β-carotene triplet state. Thus, the triplet state of β-carotene in aggregates with BChl *c* is not only produced with a high yield, but also on a picosecond timescale and is most probably populated by singlet homo-fission (see Discussion). The lifetime of the β-carotene triplet state was observed to depend on the molar ratio of β-carotene to BChl *c*, being shorter for higher concentrations of β-carotene (~2.3 μs for a molar ratio of 0.3:1, 1.8 μs for a molar ratio of 0.8:1 and 1.2 μs for a molar ratio of 1.4:1).

Discussion

In this work BChl *c* aggregates with incorporated β-carotene have been studied. The natural mixture of the four C8 and C12 homologues (together with the C31 diasteroselectivity) of BChl *c* has been used. It is known that such a mixture produces aggregates with spectral properties similar to the BChl *c* aggregates in chlorosomes. In contrast, individual C8 and C12 homologues or separated 31-R and 31-S epimers produce aggregates with different spectral properties depending remarkably on the degree of alkylation in C8 and C12 or the selected C31 diasteroisomer [30,48-50]. As one of our objectives in this study was to understand the carotenoid-BChl interactions in chlorosomes, the four main homologues of BChl *c* were used in same ratio as they are naturally found in chlorosomes.

Our results show that β-carotene interacts with BChl *c*, induces the aggregation of BChl *c* and remains embedded in the aggregates in a way similar to chlorobactene [24]. However, in comparison to chlorobactene, a higher molar ratio of β-carotene to BChl *c* is needed to achieve the same red shift of the BChl *c* Q_y absorption band. For example, a molar ratio of ~0.3:1 for β-carotene to BChl *c* yields a small red shift (715 nm), while five times lower ratio (0.06:1) gives a large shift (730 nm) when using chlorobactene. We suggest that the ϕ-end-group of chlorobactene is better suited for inducing aggregation of BChl than the β-end-group. This may indicate a role of π-π interaction for the assembly between BChl and carotenoid molecules. One of the differences between the end rings is that the C16 and C17 methyl groups of β-end-group are out-of-plane, in contrast to the in-plane methyl groups of the ϕ-end-group (Figure 1). The latter configuration would favor π-π stacking interaction between the end ring of the carotenoid and the polar chlorin ring. Because of the lack of a protein matrix, the π-π interaction is likely to govern the arrangement of the polar head of BChl and the end ring of carotenoid in aggregates, and also in chlorosomes.

Incorporation of β-carotene into aggregates is further proved by observation that pure β-carotene precipitates in aqueous buffer. The absorption spectrum taken before precipitation shows a significant blue shift (compared to that of β-carotene in THF) that is reminiscent of formation of H-aggregates [51]. In contrast, β-carotene incorporated into aggregates undergoes a red shift compared to β-carotene in THF. This change can be visualized by subtracting the spectrum of BChl *c* dimers (Figure 2a, solid line) from the spectrum of aggregates of BChl *c* with β-carotene. The difference spectra are summarized in Figure 2b. From experiments with BChl *c* aggregates with quinones [31] we know that the changes in the Soret band upon aggregation are less pronounced than those in the Q_y band. So we can conclude that the main part of the changes observed between 350-650 nm is due to the carotenoid contribution.

It is tempting to attribute the red shift to formation of J-aggregates of β-carotene in the aggregates with BChl *c*, however, the absence of annihilation in the kinetics recorded at the S_1-S_n band of β-carotene (Figure 5) rather contradicts this assignment because annihilation is usually present in excited state processes of molecular aggregates [52]. If the red shift of the β-carotene absorption band is not due to J-aggregates, other options are a shift due to dispersive interactions caused by change of polarizability [53] inside the aggregates or change of the torsional angle of the β-end-group in aggregates, due to interactions with BChl *c*. The latter would lead to a longer effective conjugation resulting in a red shift of the absorption spectrum and shorter S_1 lifetime. Yet another explanation of the red shift could involve

exciton interaction between β-carotene and BChl *c*; however, the results of our femtosecond spectroscopy experiments, which show no carotenoid signal upon BChl excitation, make this explanation unlikely.

Nevertheless, a close contact between β-carotene and BChl *c* within the aggregates is evidenced by energy transfer from the S_2 state of β-carotene. In fact, the results of transient absorption measurements reported here are similar to the ones observed in native chlorosomes [14], indicating comparable arrangement of carotenoid and BChl molecules. As in chlorosomes, the S_2-mediated energy transfer pathway is active in our aggregates. If we suppose that the shortening of the β-carotene S_2 state lifetime from ~150 fs in solution (average lifetime of the values between 120 and 180 fs reported in [53]) to 100 fs in aggregates (average value) is only due to singlet energy transfer, then it means that approximately one third of the S_2 state population is transferred to BChl *c*.

The rest of the excitation from the S_2 state of β-carotene populates the S_1 state via internal conversion. The main decay component obtained from both single kinetic fitting and global analysis was about 6 ps, which is shorter than the S_1 state lifetime of β-carotene in solution (~10 ps) [47]. This shortening corresponds to ~40% of the S_1 state population relaxing through another channel(s). Effect of environment can hardly be responsible for such a change, because the S_1 lifetime of β-carotene is essentially insensitive to solvent properties [54]. It is known that aggregation of carotenoids induces changes in the S_1 lifetime and the decay becomes non-exponential due to annihilation [51]. Although the 6 ps lifetime observed here is comparable with the 5 ps component detected in J-aggregates of zeaxanthin [51], a carotenoid with spectroscopic properties nearly identical to those of β-carotene, the absence of annihilation in the intensity-dependent kinetics shown in Figure 5 makes aggregation of β-carotene as the reason for the S_1 lifetime shortening very unlikely. Moreover, J-aggregates also contain a substantial time component of ~30 ps [51] that has not been observed in our experiments.

Another possibility how to explain the shorter S_1 state lifetime of β-carotene is energy transfer from this state to BChl *c*. The 6 ps component has a significant, although negative, contribution within the Q_y region of BChl *c* that can be associated with energy transfer from the carotenoid S_1 state, under the condition that BChl *c* decays faster than the carotenoid S_1 state. However, as the contribution is negative, it can also be due annihilation processes within BChl *c* aggregates. Energy transfer via the S_1 channel is a less likely explanation as it was observed to be negligible in both chlorosomes [14] and other natural antenna systems (CP43, CP47, PSI) utilizing β-carotene as a light-harvesting pigment [55,56]. An exception is

PSI of cyanobacteria where energy transfer with an efficiency of about 30% from the S_1 state of β-carotene to chlorophyll has been reported [57]. This relatively high efficiency was ascribed to β-carotene molecules that exhibit favorable π-π stacking with nearby chlorophylls. As discussed above, β-carotene is less suited for inducing aggregation of BChl *c* than chlorobactene and therefore the strength of the π-π (or CH-π) stacking interaction is expected to be weak in BChl aggregates with β-carotene, making energy transfer from the β-carotene S_1 state less efficient. Thus we conclude that the S_1-mediated pathway, if present at all, is only minor and cannot account for the observed shortening of the S_1 lifetime.

Since we have shown that β-carotene triplet is generated with an unusually high yield when β-carotene is embedded in BChl *c* aggregates, this triplet formation is another candidate for the additional decay channel. Assuming that the extinction coefficient of the T_1-T_n transition in aggregate is the same as the value of ~2×10^5 $M^{-1}cm^{-1}$ in organic solvents (approximate average extinction coefficient of the values reported in [58]), it is comparable to that of the S_0-S_2 transition [41,42]. Then, comparing magnitudes of the ground state bleaching and S_1-S_n transitions of β-carotene in solution [59], we can estimate that the S_1-S_n transition in β-carotene has an extinction coefficient about twice of that of the S_0-S_2 absorption, resulting in ratio of extinction coefficients $\varepsilon_{(S1\text{-}Sn)}/\varepsilon_{(T1\text{-}Tn)} \approx 1.4$. Because the magnitude of the residual signal corresponding to the triplet state (spectrum recorded at 44 ps shown in Figure 4) is about four times weaker than the maximal signal of the S_1-S_n transition (spectrum recorded at 0.5 ps in Figure 4), it implies that approximately 35% of the S_1 population would have to be converted to the triplet state to generate the T_1-T_n signal with the observed magnitude. This value agrees well (given the rough estimation of the extinction coefficients) with the approximate estimate of the 40% efficiency expected for the additional channel responsible for the shortening of the S_1 lifetime.

We therefore conclude that the shorter S_1 lifetime of β-carotene in aggregate is due to unusually high yield of triplet population that produces the β-carotene triplet state with ~40% efficiency. Although such yield is a few orders of magnitude larger than for β-carotene in solution [47], it is not an unprecedented phenomenon. The triplet yield as high as 35% has been observed for the carotenoid spirilloxanthin when bound to the light-harvesting protein LH1 of purple bacteria [60]. Binding of carotenoids to proteins proved to be the key condition for the high-yield triplet generation, as a few other examples, though with <15% yields, have been reported so far [60-62]. The triplet state is generated via a homo-fission process, in which the carotenoid singlet S_1 state (that is formally a doubly-excited state consisting of two triplet excitations coupled to an overall singlet state) breaks down to form a T_2 state (with the

energy close to the S_1 state) that rapidly decays to the lowest triplet state T_1. The crucial factor promoting the triplet fission is a distortion of the conjugated backbone induced by the binding site in protein that facilitates the break-up of the singlet state [60]. In chlorosomes, carotenoids are located within a hydrophobic space (thickness 1-3 nm) between lamellar layers, which is occupied by interdigitated esterifying alcohols of BChls [19]. In the aggregates of BChl *c* with β-carotene studied here, the organization within the aggregate is expected to be similar and probably constrains the β-carotene (length ~3 nm) molecules to adopt a specific conformation that allows for efficient triplet fission. Further argument in favor of the homo-fission mechanism is that formation of the triplet state is too fast to proceed via intersystem crossing, either from the S_1 state of β-carotene, or from the S_1 state of BChl *c* followed by triplet-triplet energy transfer. The latter is further excluded by the fact that the triplet state of β-carotene is not observed after selective excitation of BChl *c* at 720 nm (Fig. 3).

However, in all cases reported so far, the precursor of the triplet fission was the so-called S* state that is most likely associated with a specific carotenoid conformation [59,63]. The S* state is usually identified via its characteristic transient absorption band located at the high-energy side of the S_1-S_n transition [59,60,63], but kinetic separation of the S* and S_1 states is possible only for carotenoids with longer conjugation lengths [64]. For β-carotene in solution, although a hint of the S* signal was observed, the S_1 and S* state lifetimes were shown to be identical [59]. Since the S_1-S_n band of β-carotene embedded in BChl *c* aggregates is broad and no distinct shoulder or separate kinetic component attributable to the S* state is observed (Figure 4), we cannot unequivocally determine whether the S* state is involved in the ultrafast triplet formation.

As described above, approximately 30% of the β-carotene excitation is transferred to BChl *c*. This process is followed by energy relaxation within the Q_y region of BChl *c*, which is most probably dominated by exciton relaxation within the S_1 state manifold of BChl aggregates. The global fitting gives a lifetime of approximately 350 fs for this process. The dominating decay component of BChl *c* had a lifetime of ~3 ps under our experimental conditions, which is certainly affected by annihilation.

In conclusion, β-carotene induces aggregation of BChl *c* and this provides the appropriate arrangement for ultrafast energy transfer from the S_2 state of β-carotene to BChl *c*. The results of transient absorption measurements are similar to those observed in native chlorosomes, including the prominent dependence of the relaxation in the BChl *c* Q_y band on the pump intensity [46], and its weak effect on carotenoid decay [14]. Figure 7 summarizes the main

relaxation and energy transfer pathways observed in aggregates of BChl *c* with β-carotene. The efficient triplet formation by singlet homo-fission mechanism is the most likely explanation of β-carotene S_1 state lifetime shortening, making energy transfer via the S_1 state to BChl *c* unlikely. Thus, we conclude that no significant energy transfer from the S_1 state of β-carotene occurs in the aggregates, and the only active energy transfer channel proceeds via the S_2 state, resulting in overall carotenoid-to-BChl energy transfer efficiency of ~30%. This agrees with the energy transfer pathways identified in chlorosomes (from *Chlorobium phaeobacteroides*), in which the carotenoids uses exclusively the S_2 pathway to transfer energy BChl *e*, though with a higher efficiency of 60-70% [14].

Acknowledgements

This study was supported by Czech Ministry of Education, Youth and Sports (projects MSM0021620835, MSM6007665808 and AV0Z50510513), Czech Science Foundation (projects 206/09/0375, 202/09/1330 and 202/09/H041), Spanish Ministry of Education and Science (project BF2007-68107-C02-02/BMC), and AVCR-CSIC joint project (project 2008CZ0004). The authors would like to thank Marcel Fuciman and Petr Hribek for technical assistance with femtosecond spectroscopy measurements, and Ivana Hunalova, Frantisek Matousek and Anita Zupcanova for their help with pigment isolation.

References

[1] J.T. Beatty, J. Overmann, M.T. Lince, A.K. Manske, A.S. Lang, R.E. Blankenship, C.L. Van Dover, T.A. Martinson, F.G. Plumley, Proc. Natl. Acad. Sci. 102 (2005) 9306.

[2] R.E. Blankenship, K. Matsuura, in: B.R. Green and W.W. Parson (Eds.), Light-harvesting antennas in photosynthesis, Kluwer Academic Publishers, Dordrecht, 2003, p. 195.

[3] N.U. Frigaard, D.A. Bryant, in: J.M. Shively (Eds.), Complex Intracellular Structures in Prokaryotes (series: Microbiology Monographs, vol. 2), Springer, Berlin, 2006, p. 79.

[4] S. Chung, D.A. Bryant, Photosynth. Res. 50 (1996) 41.

[5] E.V. Vassilieva, V.L. Stirewalt, C.U. Jakobs, N.U. Frigaard, K. Inoue-Sakamoto, M.A. Baker, A. Sotak, D.A. Bryant, Biochemistry 41 (2002) 4358.

[6] L.A. Staehelin, J.R. Golecki, G. Drews, Biochim. Biophys. Acta 589 (1980) 30.

[7] P.G. Sorensen, R.P. Cox, M. Miller, Photosynth. Res. 95 (2008) 191.

[8] N.U. Frigaard, S. Takaichi, M. Hirota, K. Shimada, K. Matsuura, Arch. Microbiol. 167 (1997) 343.

[9] R.J. van Dorssen, P.D. Gerola, J.M. Olson, J. Amesz, Biochim. Biophys. Acta 848 (1986) 77.

[10] J. Psencik, G.F.W. Searle, J. Hala, T.J. Schaafsma, Photosynth. Res. 40 (1994) 1.

[11] J.B. Arellano, T.B. Melo, C.M. Borrego, J. Garcia-Gil, K.R. Naqvi, Photochem. Photobiol. 72 (2000) 669.

[12] T.B. Melo, N.U. Frigaard, K. Matsuura, K.R. Naqvi, Spectrochim Acta A Mol Biol Spectrosc 56 (2000) 2001.

[13] D. Carbonera, E. Bordignon, G. Giacometti, G. Agostini, A. Vianelli, C. Vannini, J. Phys. Chem. B 105 (2001) 246.

[14] J. Psencik, Y.Z. Ma, J.B. Arellano, J. Garcia-Gil, A.R. Holzwarth, T. Gillbro, Photosynth. Res. 71 (2002) 5.

[15] H. Kim, H. Li, J.A. Maresca, D.A. Bryant, S. Savikhin, Biophys. J. 93 (2007) 192.

[16] M. Foidl, J.R. Golecki, J. Oelze, Photosynth. Res. 54 (1997) 219.

[17] T.P. Ikonen, H. Li, J. Psencik, P.A. Laurinmaki, S.J. Butcher, N.U. Frigaard, R.E. Serimaa, D.A. Bryant, R. Tuma, Biophys. J. 93 (2007) 620.

[18] J. Psencik, T.P. Ikonen, P. Laurinmäki, M.C. Merckel, S.J. Butcher, R.E. Serimaa, R. Tuma, Biophys. J. 87 (2004) 1165.

[19] J. Psencik, J.B. Arellano, T.P. Ikonen, C.M. Borrego, P.A. Laurinmaki, S.J. Butcher, R.E. Serimaa, R. Tuma, Biophys. J. 91 (2006) 1433.

[20] G.T. Oostergetel, M. Reus, A. Gomez Maqueo Chew, D.A. Bryant, E.J. Boekema, A.R. Holzwarth, FEBS Lett. 581 (2007) 5435.

[21] S. Ganapathy, G.T. Oostergetel, P.K. Wawrzyniak, M. Reus, A.G.M. Chew, F. Buda, E.J. Boekema, D.A. Bryant, A.R. Holzwarth, H.J.M. de Groot, Proc. Natl. Acad. Sci. 106 (2009) 8525.

[22] A. Egawa, T. Fujiwara, T. Mizoguchi, Y. Kakitani, Y. Koyama, H. Akutsu, Proc. Natl. Acad. Sci. 104 (2007) 790.

[23] T. Jochum, C.M. Reddy, A. Eichhofer, G. Buth, J. Szmytkowski, H. Kalt, D. Moss, T.S. Balaban, Proc. Natl. Acad. Sci. 105 (2008) 12736.

[24] P. Klinger, J.B. Arellano, F.E. Vacha, J. Hala, J. Psencik, Photochem. Photobiol. 80 (2004) 572.

[25] T. Miyatake, H. Tamiaki, J. Photochem. Photobiol. C 6 (2005) 89.

[26] T.S. Balaban, H. Tamiaki, A.R. Holzwarth, Top. Curr. Chem. 258 (2005) 1.

[27] H. Tamiaki, R. Shibata, T. Mizoguchi, Photochem. Photobiol. 83 (2007) 152.

[28] A. Zupcanova, J.B. Arellano, D. Bina, J. Kopecky, J. Psencik, F. Vacha, Photochem. Photobiol. 84 (2008) 1187.

[29] M. Hirota, T. Moriyama, K. Shimada, M. Miller, J.M. Olson, K. Matsuura, Biochim. Biophys. Acta 1099 (1992) 271.

[30] D.B. Steensgaard, H. Wackerbarth, P. Hildebrandt, A.R. Holzwarth, J. Phys. Chem. B 104 (2000) 10379.

[31] J. Alster, A. Zupcanova, F. Vacha, J. Psencik, Photosynth. Res. 95 (2008) 183.

[32] T. Miyatake, H. Tamiaki, A.R. Holzwarth, K. Schaffner, Helvetica Chimica Acta 82 (1999) 797.

[33] T. Miyatake, H. Tamiaki, M. Fujiwara, T. Matsushita, Bioorg. Med. Chem 12 (2004) 2173.

[34] Y. Saga, S. Akai, T. Miyatake, H. Tamiaki, Bioconjugate Chemistry 17 (2006) 988.

[35] V.I. Prokhorenko, A.R. Holzwarth, M.G. Muller, K. Schaffner, T. Miyatake, H. Tamiaki, J. Phys. Chem. B 106 (2002) 5761.

[36] B. Zietz, V.I. Prokhorenko, A.R. Holzwarth, T. Gillbro, J. Phys. Chem. B 110 (2006) 1388.

[37] C. Roger, M.G. Muller, M. Lysetska, Y. Miloslavina, A.R. Holzwarth, F. Wurthner, J. Am. Chem. Soc. 128 (2006) 6542.

[38] A. Huijser, P.L. Marek, T.J. Savenije, L.D.A. Siebbeles, T. Scherer, R. Hauschild, J. Szmytkowski, H. Kalt, H. Hahn, T.S. Balaban, J. Phys. Chem. C 111 (2007) 11726.

[39] K. Schmidt, Arch. Microbiol. 124 (1980) 21.

[40] R.Y. Stanier, J.H.C. Smith, Biochim. Biophys. Acta 41 (1960) 478.

[41] F.H. Foppen, Chromatogr. Rev. 14 (1971) 133.

[42] A. Young and G. Britton, Carotenoids in Photosynthesis, Chapman & Hall, London, 1993.

[43] I.H.M. van Stokkum, D.S. Larsen, R. van Grondelle, BBA-Bioenergetics 1658 (2004) 262.

[44] M. Umetsu, R. Seki, T. Kadota, Z.Y. Wang, T. Adschiri, T. Nozawa, J. Phys. Chem. B 107 (2003) 9876.

[45] F.L. de Weerd, I.H.M. van Stokkum, R. van Grondelle, Chem. Phys. Lett 354 (2002) 38.

[46] J. Psencik, Y.Z. Ma, J.B. Arellano, J. Hala, T. Gillbro, Biophys. J. 84 (2003) 1161.

[47] T. Polivka, V. Sundstrom, Chem. Rev. 104 (2004) 2021.
[48] K. Uehara, M. Mimuro, Y. Ozaki, J.M. Olson, Photosynth. Res. 41 (1994) 235.
[49] T. Mizoguchi, K. Hara, H. Nagae, Y. Koyama, Photochem. Photobiol. 71 (2000) 596.
[50] T.S. Balaban, Acc. Chem. Res. 38 (2005) 612.
[51] H.H. Billsten, V. Sundstrom, T. Polivka, J. Phys. Chem. A 109 (2005) 1521.
[52] G. Trinkunas, J.L. Herek, T. Polivka, V. Sundstrom, T. Pullerits, Phys. Rev. Lett. 86 (2001) 4167.
[53] A.N. Macpherson, T. Gillbro, J. Phys. Chem. A 102 (1998) 5049.
[54] P.O. Andersson, S.M. Bachilo, R.L. Chen, T. Gillbro, J. Phys. Chem. 99 (1995) 16199.
[55] F.L. de Weerd, J.P. Dekker, R. van Grondelle, J. Phys. Chem. B 107 (2003) 6214.
[56] N.E. Holt, J.T.M. Kennis, G.R. Fleming, J. Phys. Chem. B 108 (2004) 19029.
[57] F.L. de Weerd, J.T.M. Kennis, J.P. Dekker, R. van Grondelle, J. Phys. Chem. B 107 (2003) 5995.
[58] B.R. Nielsen, K. Jorgensen, L.H. Skibsted, J. Photochem. Photobiol. A-Chem. 112 (1998) 127.
[59] P. Chabera, M. Fuciman, P. Hribek, T. Polivka, Physical Chemistry Chemical Physics in press (2009
[60] C.C. Gradinaru, J.T.M. Kennis, E. Papagiannakis, I.H.M. van Stokkum, R.J. Cogdell, G.R. Fleming, R.A. Niederman, R. van Grondelle, Proc. Natl. Acad. Sci. 98 (2001) 2364.
[61] E. Papagiannakis, I.H.M. van Stokkum, M. Vengris, R.J. Cogdell, R. van Grondelle, D.S. Larsen, J. Phys. Chem. B 110 (2006) 5727.
[62] T. Polivka, S.P. Balashov, P. Chabera, E.S. Imasheva, A. Yartsev, V. Sundstrom, J.K. Lanyi, Biophys. J. 96 (2009) 2268.
[63] D.M. Niedzwiedzki, J.O. Sullivan, T. Polivka, R.R. Birge, H.A. Frank, J. Phys. Chem. B 110 (2006) 22872.
[64] T. Polivka, V. Sundstrom, Chem. Phys. Lett 477 (2009) 1.

Figure legends

Figure 1

Molecular structure of the main chlorosomal carotenoids: (a) chlorobactene, (b) isorenieratene (c) β-carotene.

Figure 2

Steady state and difference absorption spectra of β-carotene and BChl *c* forms. (a) Absorption spectra of BChl *c* aggregates with β-carotene for different molar ratios. Spectra were normalized at 340 nm and offset for the sake of clarity. Vertical line at 715 nm is drawn to facilitate comparison. (b) Difference spectra between the aggregates (patterned lines in panel a) and BChl *c* dimers (solid line in panel a). (c) Absorption spectrum of β-carotene dissolved in tetrahydrofuran (solid line), Tris-HCl buffer (dashed line) and inside the aggregates (dash-dotted line, reproduced from panel b).

Figure 3

Transient absorption spectra of BChl *c* aggregates with β-carotene at several delays after excitation at 720 nm. Lines were smoothed by adjacent averaging. Rescaled inverted steady state absorption spectra are shown for the sake of comparison.

Figure 4 (color figure)

Transient absorption and decay associated spectra after excitation at 520 nm. (a) Transient absorption spectra of BChl *c* aggregates with β-carotene at several delays. (b) Decay associated spectra for the lifetime components resolved by global analysis. Lines in both panels were smoothed by adjacent averaging. Rescaled inverted steady state absorption spectra are shown in both panels for the sake of comparison.

Figure 5

Pump intensity dependence of the kinetic traces of BChl *c* aggregates with β-carotene probed at (a) 592 nm and (b) 752 nm after excitation at 490 nm. Intensities are in photons $pulse^{-1}$ cm^{-2}. All curves are normalized.

Figure 6

Decay associated spectrum for the 2.3 μs component of BChl *c* aggregates with β-carotene (solid line) and the inverted and rescaled β-carotene steady state absorption spectrum in aggregates (dashed line), obtained in the same way as spectra in Figure 2b.

Figure 7

Scheme summarizing the relaxation and energy transfer pathways in BChl *c* aggregates with

β-carotene, after β-carotene excitation. IC, internal conversion; HF, homo-fission; A, absorption; F, fluorescence; ET, energy transfer.

Figure(s)

Click here to download high resolution image

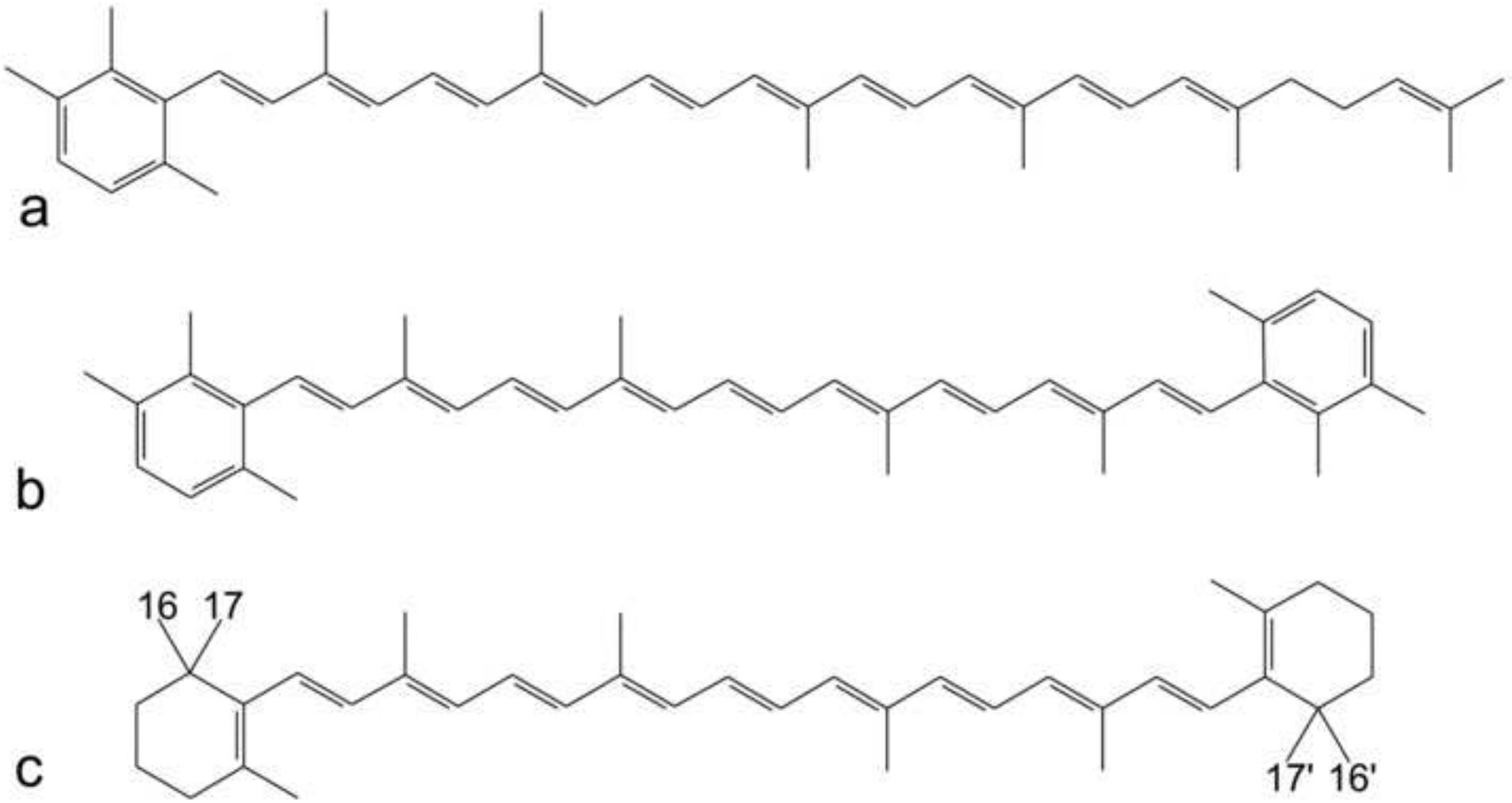

Figure(s)

Click here to download high resolution image

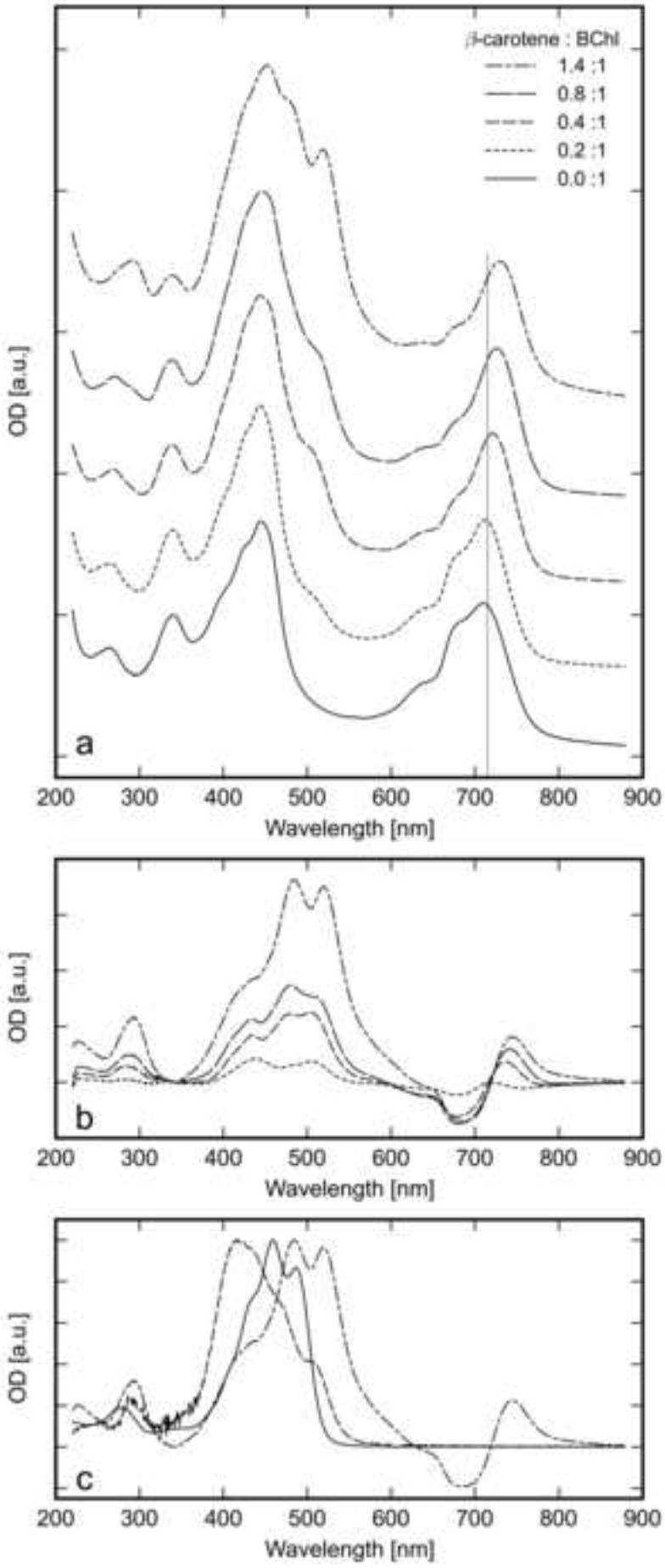

Figure(s)

Click here to download high resolution image

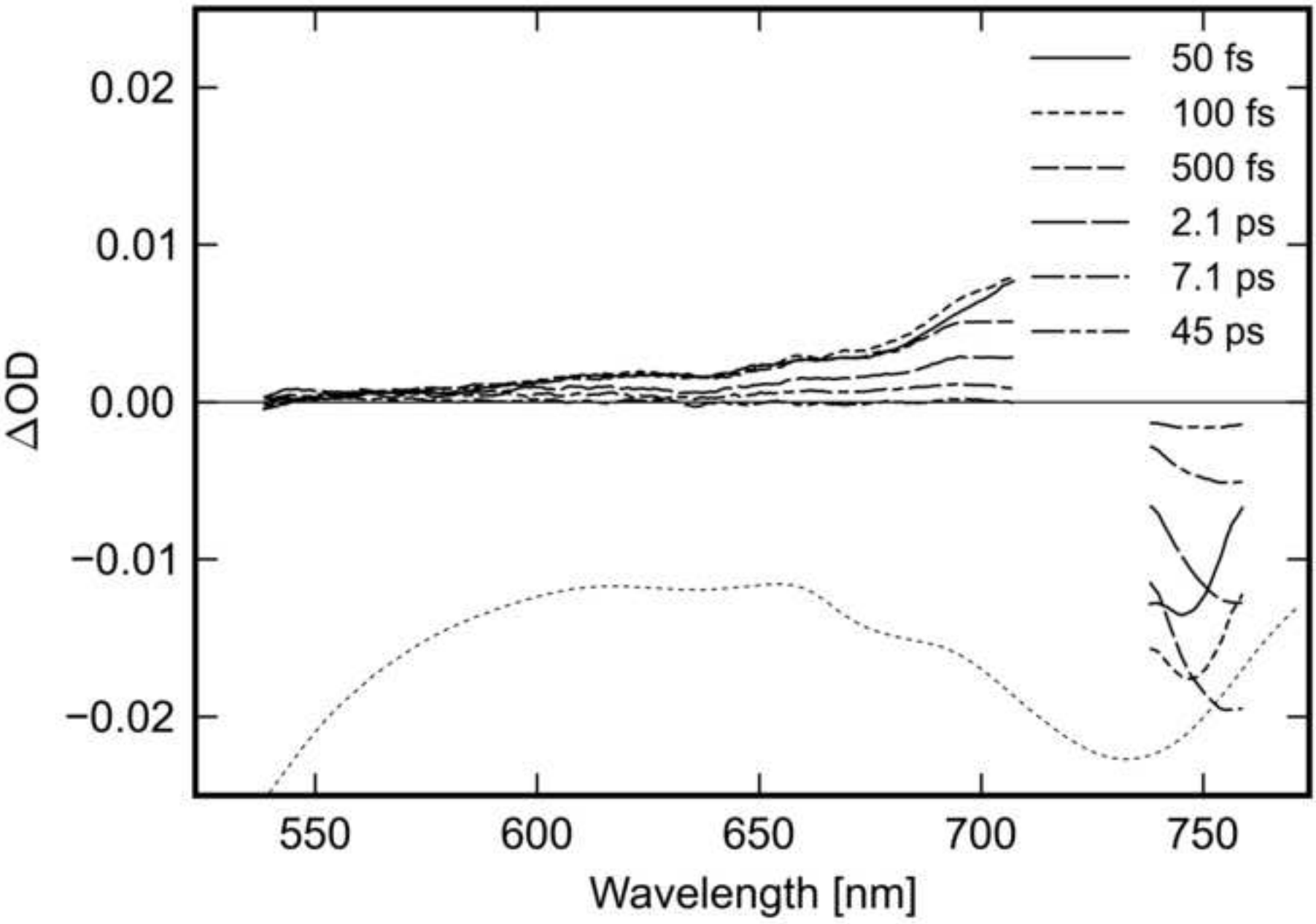

Figure(s)
Click here to download high resolution image

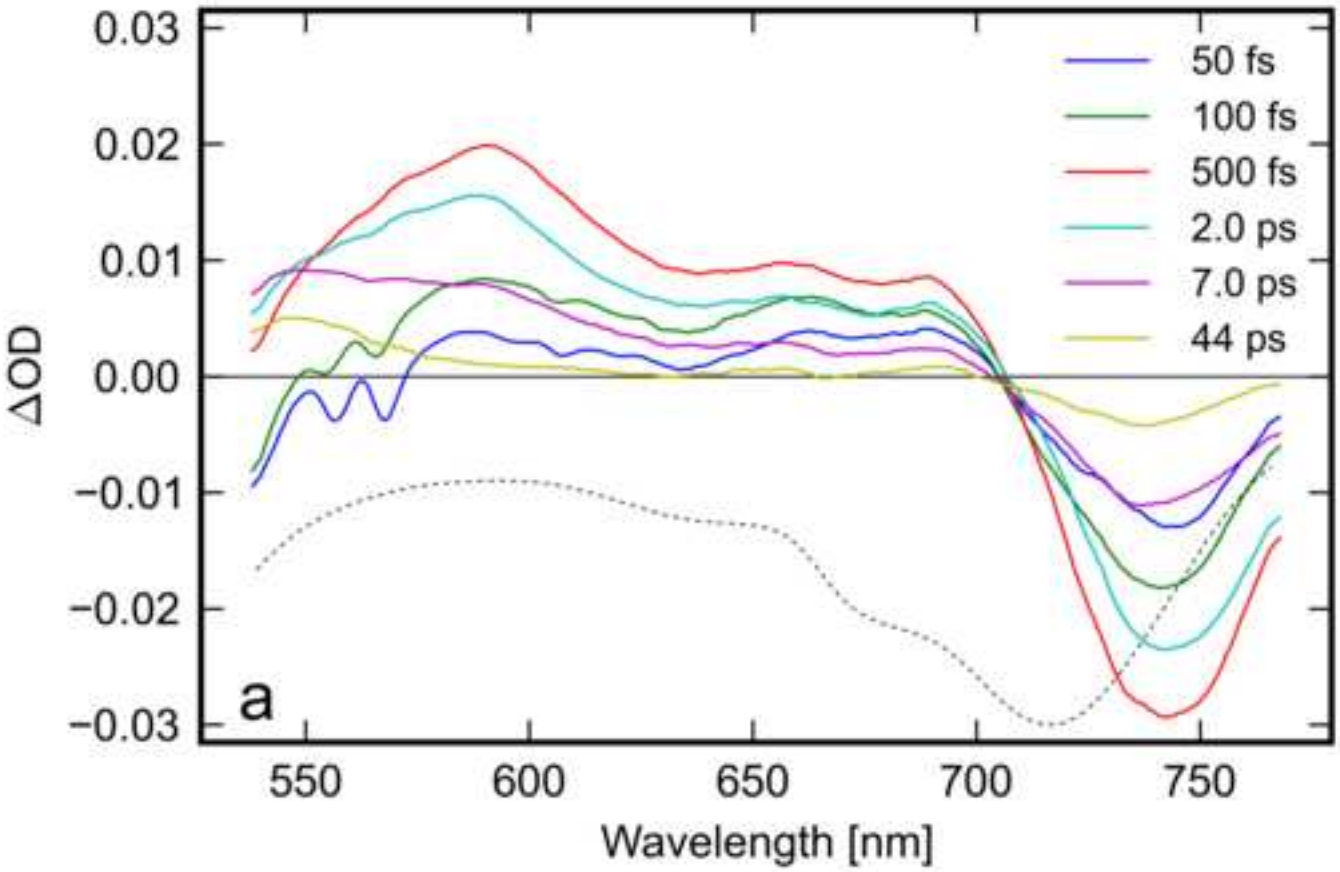

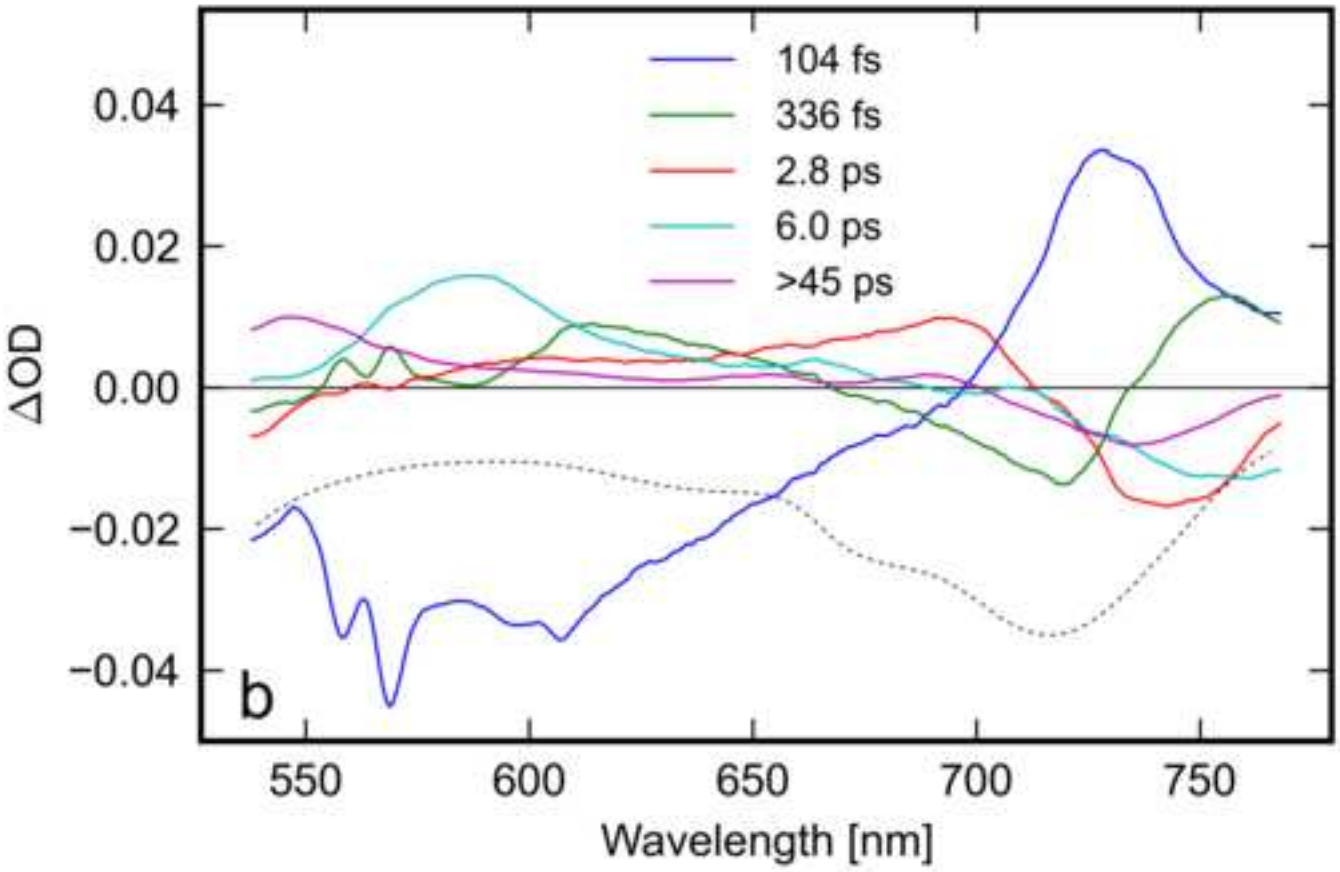

Figure(s)
Click here to download high resolution image

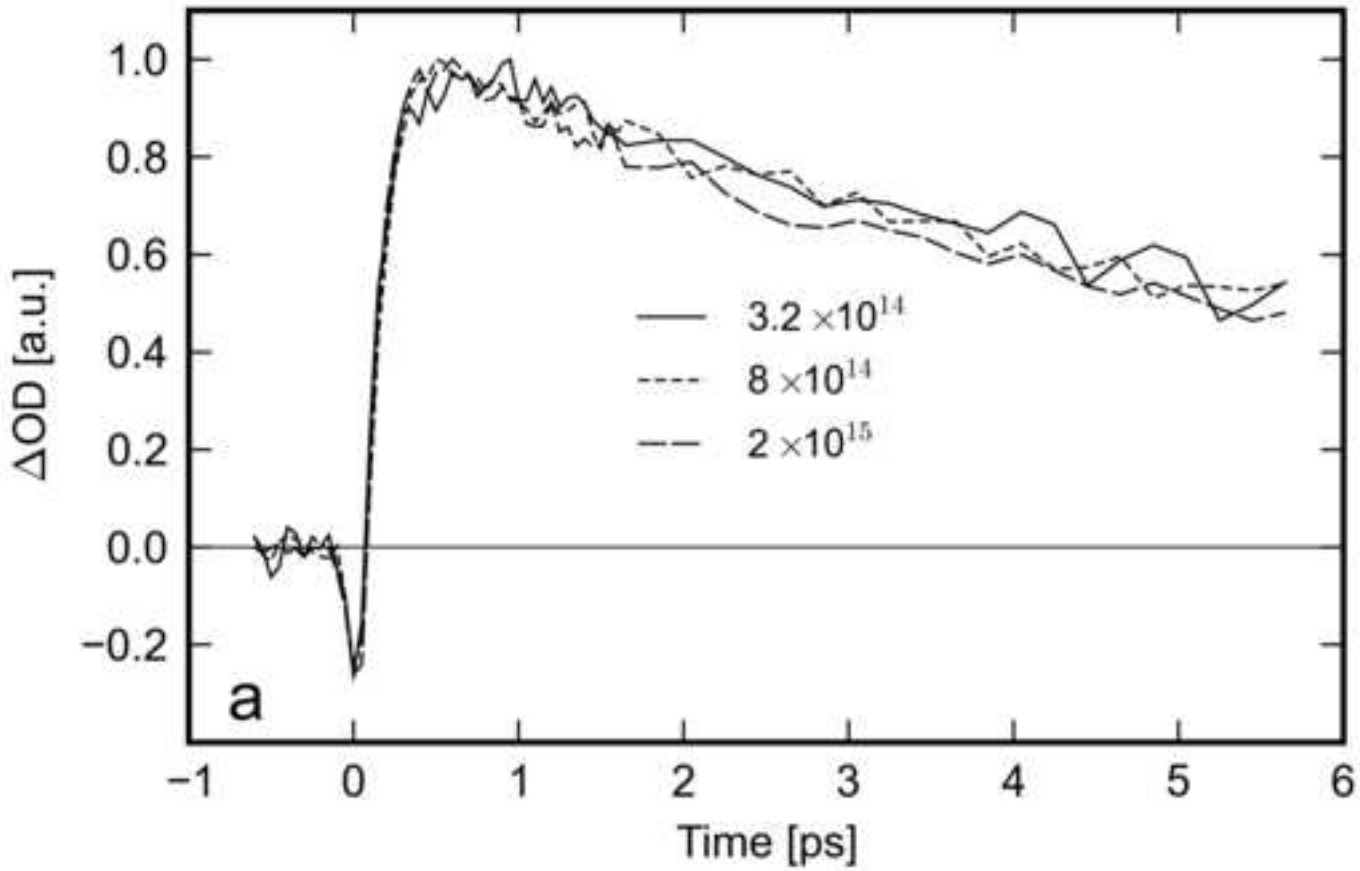

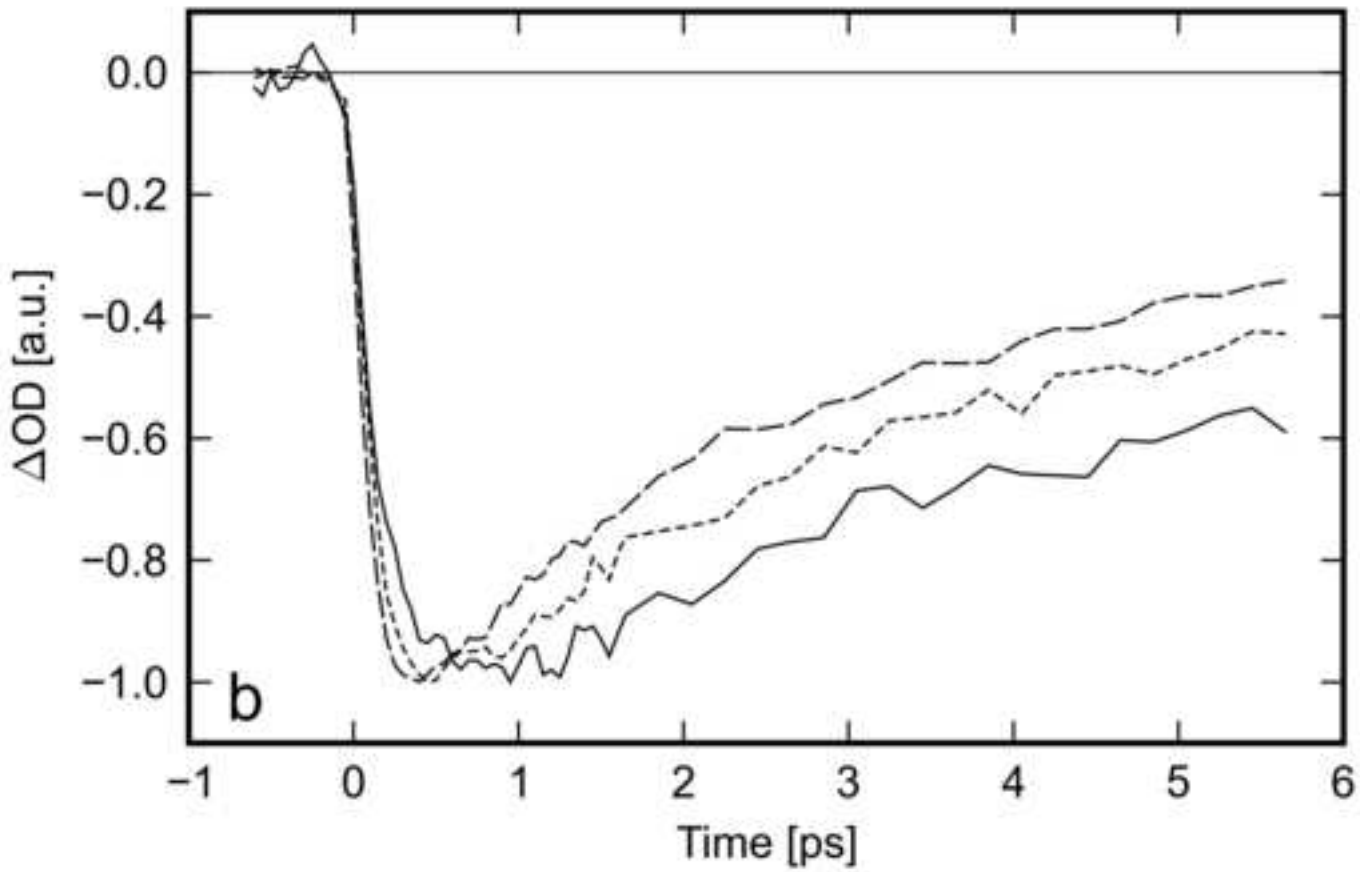

Figure(s)

Click here to download high resolution image

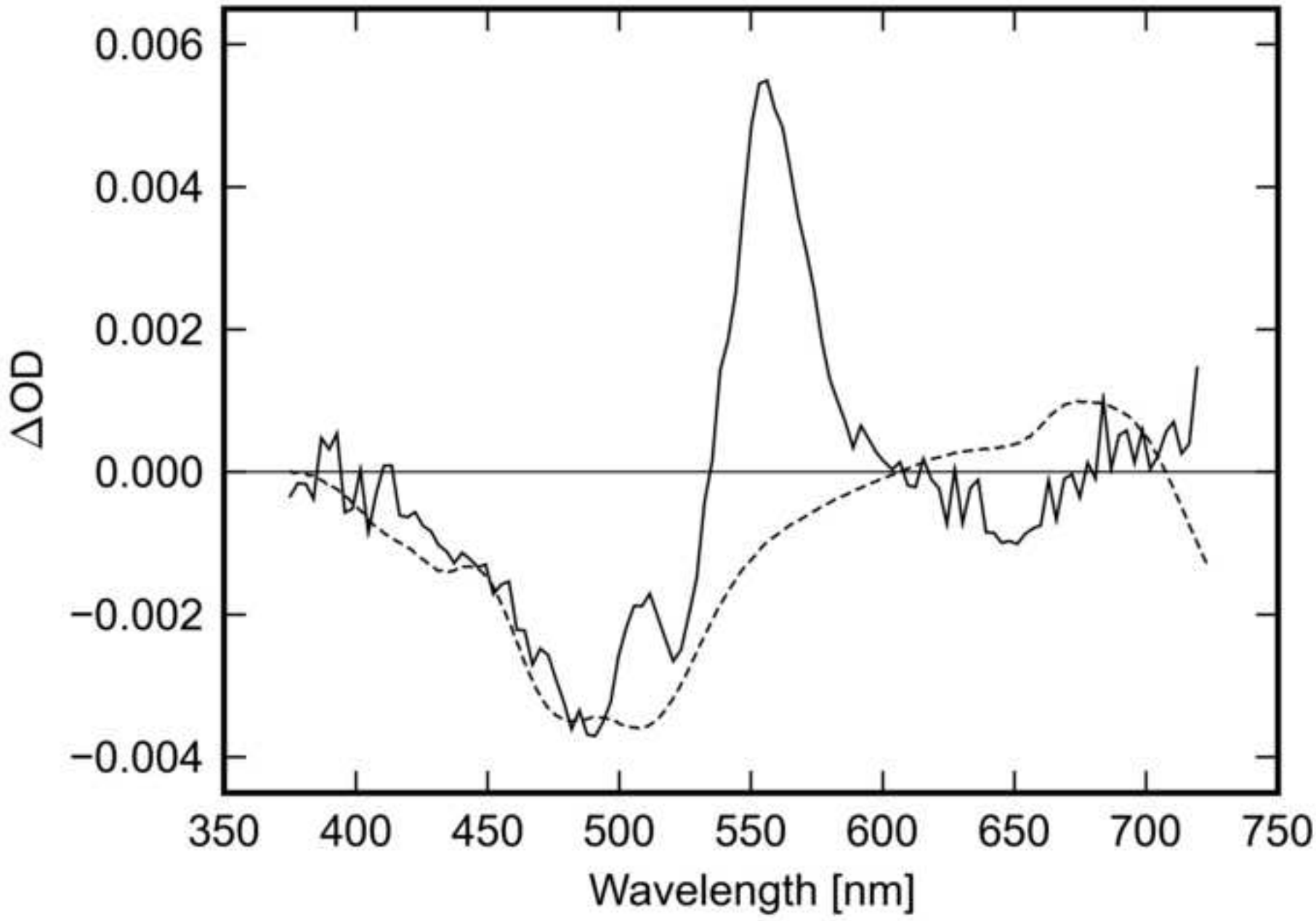

Figure(s)

Click here to download high resolution image